

PASSIVE ANTI-ICING SYSTEM USING PASS-THROUGH EVAPORATOR CAPILLARY PUMPED LOOP

Romain Rioboo⁽¹⁾, Anthony Chartier⁽¹⁾, Stéphane Van Oost⁽¹⁾, Mikael Mohaupt⁽¹⁾, Ana-Belen Blanco Maroto⁽²⁾, Francisco-José Redondo Carracedo⁽²⁾ & Laurent Barremaecker⁽¹⁾

⁽¹⁾ Euro Heat Pipes, Rue de l'industrie 24, 1400 Nivelles (Belgium), rri@ehp.be

⁽²⁾ Airbus DS, Avenida John Lennon, s/n, 28609 Getafe (Spain), francisco.r.redondo@airbus.com

KEYWORDS: Capillary Pumped Loop, Anti-Icing, Engine Air Intake, passive heat transfer, high efficiency

ABSTRACT:

This work presents the development of an anti-icing system that utilizes a two-phase passive system to bring the heat power from pressurised hot air present in the vicinity of the engine, to the surface of the engine air intake to protect it against icing. A full scale model has been built and tested in laboratory conditions to validate the concept and assess its efficiency.

1. INTRODUCTION

Preventing the icing of the Engine Air Intake (EAI) of turbo-propeller is a key issue to guarantee the good operation of powerplants and safety of airplanes. Currently the techniques mainly used consist in heating the icing zones of the EAI using either electrical resistances or injecting hot air on the backside of the surface to protect. A de-icing based on pneumatic rubber boots is also used.

In order to comply with the airplane regulation [1] several key parameters are to be met with multiple engineering cases depending on the atmospheric, flight and engine conditions. Among these, several are demanding a large amount of power to be transported. In our case, the surface to protect of the EAI must be kept above 40°C while outside temperature may vary strongly, possibly with very cold temperatures such as -40°C for example. Another key specification was that the power to be transported can reach values up to 7 kW.

The cold source is the icing cold air impacting the EAI surface while the hot source is pressurized hot air, available in the vicinity of the EAI, from which wasted energy can be extracted.

The project which is described here, proposes to develop a system that can meet the specification using a passive two-phase capillary loop to

transport the power from the hot source to the cold source and, in this way, keep the surface to protect of the EAI at the desired temperature.

The proposed work will mimic hot and cold source of the real application to validate the possibility to use a two-phase thermal transfer system using passive capillary loop for an anti-icing system.

Several two-phase systems (Loop Heat Pipes, LHP) have already been used to heat the surface to protect of an EAI for drones [2; 3; 4] or at laboratory level [5, 6]. All these systems, which are transferring 1.5 kW at most per LHP [4], utilize LHP technology on which the hot source environment is influencing the saturation temperature because the evaporator and the reservoir are hydraulically and thermally connected. Despite these limitations, these successful tests in icing conditions [2], open the way of using the highly efficient technology of passive loop for heat transfer in anti-icing applications.

In the present study a Capillary Pumped Loop (CPL) is used. The identified hot source is, in the application, not too far from the surface to protect and composed of compressed hot air flowing at given mass flow rates and temperatures depending on flight situation. The hot air thermal energy is transferred to the double-sided evaporator of the CPL through finned heat exchangers where the working fluid (methanol) evaporates at saturation temperature (T_{sat}). The vapor is passively pushed to the condenser consisting of a dedicated tube network covering the EAI surface to protect from icing. Figure 1 shows schematically the concept developed in this study.

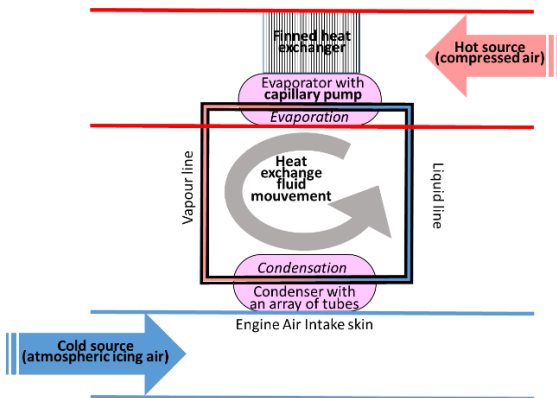


Figure 1: Scheme of the technology to transfer heat from the available hot source to the EAI surface to protect by heating

2. SPECIFICATIONS

The available hot source was specified to be pressurized hot air flowing in an accessible pipe at various temperatures and mass flow rates, while the cold source was the aluminum engine air intake surface to be protected against icing, divided into 5 zones (Zi: Z1 to Z5, see Figure 2) submitted at various temperatures, power densities, q_{Zi} , and power, Q_{Zi} , as a result of the cold air and the icing droplet reaching the EAI surface to protect.



Figure 2: Engine Air Intake. Top: EAI of a turbo-propeller engine. Bottom: the five zones of the surface to protect of the EAI

The specifications were derived from [1] and various flight and engine conditions. While the total area of the 5 zones of the surface to protect of the EAI is of 0.89 m^2 , the volume of the evaporator

shall be as low as possible considering it must be integrated in the engine nacelle. The system must sustain permanently 2g acceleration in all direction.

A total of 34 design cases were investigated. Minimum and maximum values of various parameters are provided in the next table (Table 1).

| Parameter | Unit | Min | Max |
|------------------------------|------|------|------|
| Hot source MFR | kg/s | 0.12 | 0.33 |
| Hot source temperature | °C | 110 | 250 |
| T_{amb} (cold source) | °C | -40 | 0 |
| T_{cold} (EAI temperature) | °C | 40 | 100 |
| Q_{Z1} (cold source) | W | 1600 | 2800 |
| Q_{Z2} (cold source) | W | 260 | 1100 |
| Q_{Z3} (cold source) | W | 440 | 1900 |
| Q_{Z4} (cold source) | W | 390 | 1600 |
| Q_{Z5} (cold source) | W | 16 | 100 |
| $Q_{total} (Z1+...+Z5)$ | W | 7198 | 3046 |

Table 1: Minimum and maximum values of main parameters which vary with design case

3. SYSTEM DESCRIPTION

In order to validate the concept, a 1:1 scale full stainless-steel pass-through evaporator CPL model was built with a flat condenser instead of a curved one. This new CPL has an evaporator with 2 porous wicks having $1.5 \mu\text{m}$ pore diameter and 45% porosity. The scheme of the CPL is presented in Figure 3.

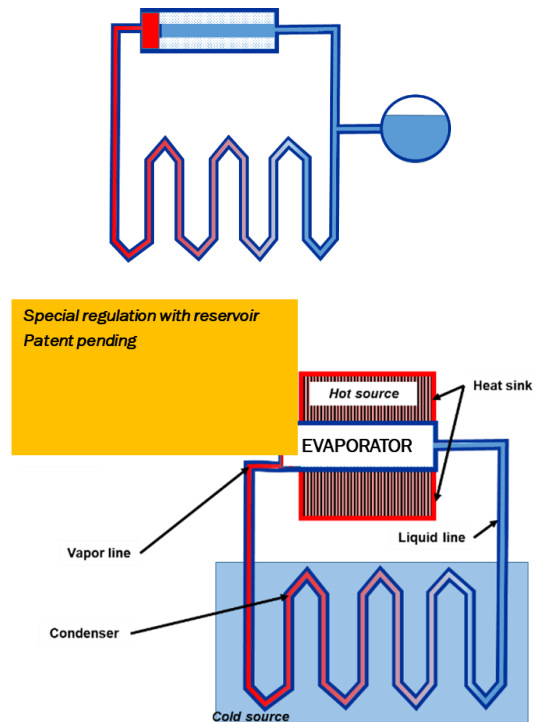


Figure 3: Scheme of CPL (Top: typical CPL; Bottom: present configuration)

The concept of the pass-through evaporator configuration has been tested in the past [7] but, to our knowledge, only for a start-up function. It enables to suppress possible instabilities of classical CPL [8, 9]. The CPL tested is presented in Figure 4 (bottom). The hot air thermal energy is transferred to the double-sided evaporator of the CPL through very high aspect ratio finned aluminum heat exchangers, where the working fluid (methanol) evaporates at saturation temperature (T_{sat}) which is controlled by a heating cartridge placed in the reservoir. The vapor is passively pushed to the condenser composed of a dedicated tubes network covering the EAI surface to protect by the heating released by condensation. The system was insulated to reduce possible losses.

The evaporator is flat and double-sided which enables a relatively large evaporation surface of $2 \times 100 \times 200 \text{ mm}^2$. The Figure 5 presents the inside view of the evaporator duct.

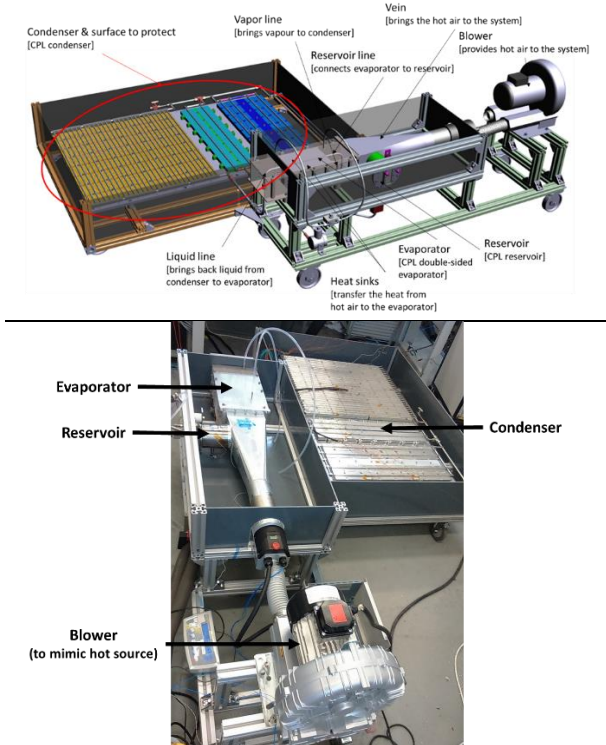


Figure 4: System description

On each side of the evaporator a linear fin heat sink is attached. Thermal paste enables a good thermal contact. The heat sink is used here to collect the heat to the evaporator instead of removing it from a hot surface. This heat exchanger was simply characterized by its thermal

resistance which varies with its dimension (see Table 2) and mass flow rate (see Table 1).

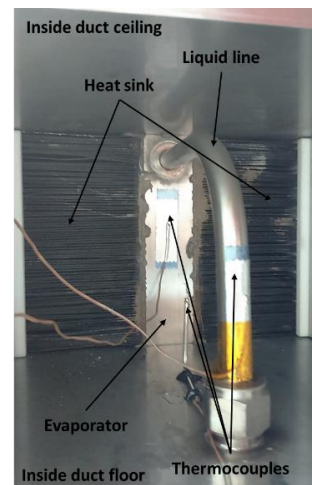


Figure 5: Inside view of the evaporator duct

The condenser is built with a distribution of vapor on every zone with a series/parallel configuration as described in Figure 6.

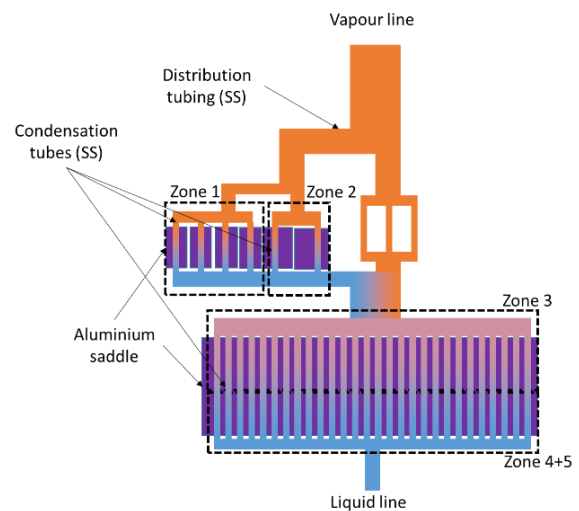


Figure 6: Scheme of the condenser distribution of vapour

In such a way, enough potential heat is reaching all zones to fulfil requirements on power and power density. The condenser was made of stainless-steel tubes glued on aluminum saddles (see Figure 7). The vapor is reaching in parallel zone 1 and 2 and 3 bypass tubes which brings directly the heat to zone 3 and its 28 tubes in parallel. The zone 4 and 5 are following zone 3, in series. The diameter of the 3 bypass tubes and the 6 condensation tubes of zones 1 & 2 are the same. On the other hand, the length is calculated to ensure similar pressure drop and thus be able to distribute $2/3^{\text{rd}}$ of

the power to zones 1 and 2 while 1/3rd to zones 3 to 5. In the same way, the length of the condensation tubes of zones 1 & 2 are equals.

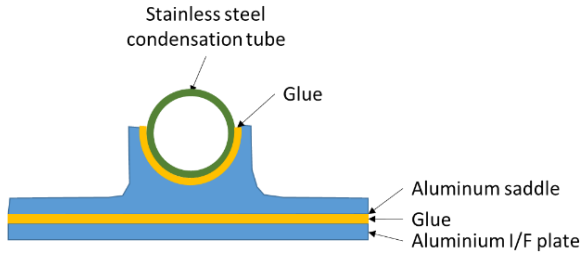


Figure 7: Scheme of the condenser tubes

Two configurations of the system (EM1 and EM2) were tested in which the effect of gravity, the type of heat sink and the heating of the reservoir was changed (see Table 2).

| Aspect | EM1 | EM2 |
|--|-------------------------------------|--------------------------------------|
| Position wrt gravity (from top to bottom) | Evaporator = reservoir Condenser | Condenser Evaporator Reservoir |
| 2 Heat sink (227x110mm) with 0.6mm fin thickness and 55mm height | 85 Linear fins | 76 slotted fins (47x5x1,1 mm slots) |
| Reservoir heating | Thermal gun | Heating cartridge |

Table 2: Configurations of the system

4. EXPERIMENTAL SET-UP

Thermocouples were implemented in all key parts of the system. The power transported is deduced from difference of temperature inside the evaporator vein just before (T_{in}) the heat sinks and just after (T_{out}). We consider that the transported power (Q_{trans}) is given by:

$$Q_{trans} = \dot{m}_{air} c_{p_{air}} (T_{in} - T_{out})$$

With \dot{m}_{air} being the MFR and $c_{p_{air}}$ the specific heat of the hot air.

Insulation of the evaporator vein enabled to neglect the losses in this zone. T_{sat} was measured by a pressure sensor connected to the reservoir.

1.1. Condenser side

The experimental set-up used a cold plate that can be controlled in temperature. Electric heaters and tubes in which liquid nitrogen is injected are distributed on the back of the cold plate. In order to fulfil the variation in power density from one zone to the other of the condenser, an aluminum I/F

plate is added between the cold plate and the aluminum saddles of the condenser. It was considered here that the cold plate is extracting heat uniformly. The I/F plate is design in such a way that the surface area between I/F plate and condenser saddle on one side, and between I/F plate and cold plate on the other side, are adjusted to fulfil requirement on power density fluxes at condenser from zone to zone (see Figure 8).

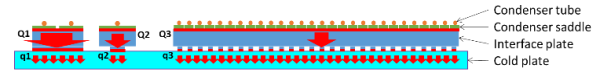


Figure 8: Scheme of the I/F plate at condenser

1.2. Evaporator side

A blower (Leister LHS 61L, 11kW) is used to mimic the hot source. It enables to provide air at a MFR up to 0.0516 kg/s for the linear fins heat sinks and 0.0634 kg/s for the slotted fins heat sinks (due to lower pressure drop) and at temperatures up to 250°C. To note these flows are lower (by far) with those indicated in Table 1.

5. RESULTS

Two series of tests have been made corresponding each one to EM1 and EM2. A first evaluation of the optimum value of T_{sat} , considering the pressure drop balance inside the CPL, enabled to assess that a T_{sat} at 80°C is the optimum in terms of quantity of power transported inside the CPL.

5.1. Test cases

The main objective of these tests was to:

- Show it can work in a stable way and not only as a start-up system;
- Demonstrate it can transport enough power for the application;
- Explore performances in function of the T_{sat} , MFR, hot source temperature.

5.2. EM1

During the first series of tests, it was not possible to adjust precisely the power injected in the reservoir to maintain the T_{sat} at the desired temperature. This was performed automatically through a thermal gun directed towards the reservoir. This method forbidden to evaluate the power injected in the fluid inside the reservoir and induced a certain delay in the control of T_{sat} , which complicated the tests. The EM2 configuration was implemented mostly to improve the issue.

The Table 3 shows the experimental results with the EM1 configuration.

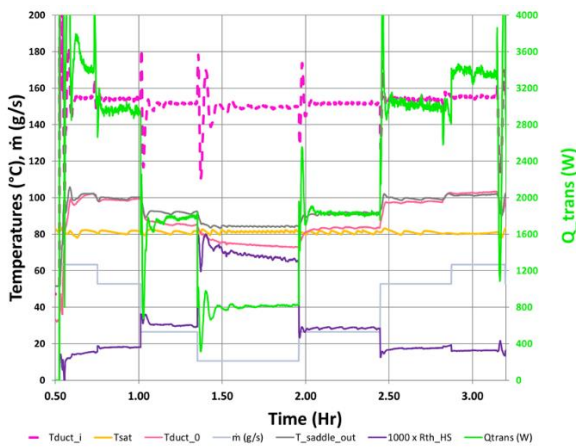
| Case | T_{hot_source} | T_{sat} | Q_{trans} |
|-------|-------------------|-----------|-------------|
| | [°C] | [°C] | [W] |
| A-exp | 142 | 81 | 1832 |
| B-exp | 147 | 80 | 1699 |
| C-exp | 154 | 90 | 1671 |
| D-exp | 155 | 70 | 2157 |
| E-exp | 114 | 81 | 728 |
| F-exp | 115 | 91 | 274 |
| G-exp | 114 | 90 | 706 |
| H-exp | 124 | 90 | 966 |
| I-exp | 123 | 71 | 1275 |
| J-exp | 196 | 90 | 2638 |
| K-exp | 192 | 71 | 2990 |

Table 3: Experimental results on transported power of EM1

Despite the low MFR achieved with the blower and the linear heat sinks, the system can transport up to 3 kW. But it can also be seen that at low power to transport (cases E, F & G) the performance in terms of transported heat of the system is low.

5.3. EM2

For this new model it was possible to implement a TC between the heat sink and the evaporator saddle to measure directly the thermal resistance of the heat sink itself (R_{th_HS}).



| MFR [kg/s] | Q_{trans} [W] | Measured R_{th_HS} [K/W] |
|------------|-----------------|-----------------------------|
| 0.0634 | 3408 | 0.015 |
| 0.0528 | 2960 | 0.018 |
| 0.0220 | 1782 | 0.03 |
| 0.0037 | 811 | 0.068 |

Figure 9: Influence of the MFR on the thermal resistance of one heat sink (with $T_{in}=150^{\circ}C$)

The implementation of a heating cartridge directly in the reservoir; enabled to compare the amount of power injected in the reservoir through the heating cartridge (Q_{res}) and the one of the power transported from the hot source to the cold source (Q_{trans}).

The influence of the MFR on the thermal resistance of the heat sink can be seen on Figure 9. The experiment was performed in first decreasing the mass flow rate and then by increasing with similar steps. The Figure 9 (top) shows the reproducibility of the results. Clearly, the thermal resistance of the heat sink is decreasing strongly with the mass flow rate. The overall measured resistance of the system is ranging from 0.0144 K/W up to 0.029 K/W, at high MFR, depending on the various parameter. It shows that at low transmitted power the thermal resistance is higher. The average value is of 0.02 K/W.

The influence of the inlet temperature and of the saturation temperature was also investigated.

| T_{in} [°C] | 112 +/-1 | 182 +/-1 | 228 +/-6 |
|----------------|----------|----------|----------|
| T_{sat} [°C] | | | |
| 70.4 +/-0.2 | 2186 | 5099 | 7199 |
| 80.7 +/-0.5 | 1797 | 4925 | 6880 |
| 89.3 +/-0.2 | 1549 | 4814 | 6175 |

Table 4: Transported power (Q_{trans}) in function of inlet temperature (T_{in}) and saturation temperature (T_{sat}) for EM2

These results show that the CPL can transport up to 7.2 kW which is compatible with the application and the specification. The power of the heater cartridge inserted in the reservoir has been measured at the same time and the typical value of the ratio between the injected power to the transported one is of 1.8%. This low ratio, added to the previous results, is again validating the application of the CPL technology for anti-icing system of EAI.

6. CONCLUSION

A full-scale thermal system to transport power from a hot flowing air to a cold icing surface with a new design has been built and tested. The experimental set-up mimics the hot source and the cold source of an engine air intake of a turbo-propeller in order to protect its icing surface. Almost passive, this system is a pass-through evaporator capillary pumped loop that can transport more than 7kW with an overall thermal resistance of 0.02 K/W. The power used to control

its saturation temperature represents less than 2% of the transported power. The study investigated the influence of various parameters and validated the potential of this technology for anti-icing applications, mostly where the hot source is close enough to the icing surface.

The work was performed under the Cleansky 2 project PIPS (Passive Ice Protection System), grant n° 717156)

7. ABBREVIATIONS AND ACRONYMS

EAI: Engine Air Intake

CPL: Capillary Pumped Loop

I/F: Interface

LHP: Loop Heat Pipe

MFR: Mass flow rate

T_{in} : Hot air temperature at the inlet of the heat sink

T_{out} : Hot air temperature at the outlet of the heat sink

T_{amb} : Ambient temperature

T_{sat} : Saturation temperature

Wrt: with respect to

8. REFERENCES

1. EASA CS-25 Certification Specifications And Acceptable Means of Compliance (Paragraph 25.1093 and App C) & EUROCAE norm. (2011) DO 160G-ED-14G Environmental Conditions and Test Procedures for Airborne Equipment.
2. Phillips, A.L. & Wert, K.L. (2000). Loop Heat Pipe Anti Icing System Development Program Summary. *SAE Technical Paper Series* 2000-01-2493.
3. Phillips, A.L. & Gernert, N.J. (1998). Passive Aircraft Anti Icing System Using Waste Heat. *SAE Technical Paper Series* 981542.
4. Su, Q., Chang, S., Zhao, Y., Zheng, H. & Dang, C. (2018) A review of loop heat pipes for aircraft anti-icing applications. *Appl. Therm. Eng.* **130**, pp 528-540.
5. Gregori, C., Mishkinis, D., Prado, P., Torres, A. & Pérez, R. (2007) Loop Heat Pipe Technology for Aircraft Anti-Icing Applications. *SAE Technical Paper Series* 2007-01-3312.
6. Su, Q., Chang, S., Song, M., Zhao, Y. & Dang, C. (2019) An experimental study on the heat transfer performance of a loop heat pipe system with ethanol-water mixture as working fluid for aircraft anti-icing. *Int. J. Heat Mass Trans.* **139**, pp 280-292.
7. Butler, D., Ottenstein, L. & Ku, J. (1996) Design Evolution of the Capillary Pumped Loop (CAPL 2) Flight Experiment. *SAE Technical Paper Series* 961431.
8. Kaled, A., Dutour, S., Platel, V., Lluc, J. (2015) Experimental study of a Capillary Pumped Loop for cooling power electronics: Response to high amplitude heat load steps. *Appl. Therm. Eng.* **130**, pp 528-540.
9. Accorinti, F., Ayel, V. & Bertin, Y. (2019) Steady-state analysis of a Capillary Pumped Loop for Terrestrial Application with methanol and ethanol as working fluids. *Int. J. Therm. Sci.* **137**, pp 571-583.